Computational Studies of Horizontal Axis Wind Turbines

Quarterly Progress Report

Covering the period

May 6, 2000 – August 30, 2000

Contract No. XCX-7-16466-02

Submitted to the

National Renewable Energy Laboratory
Attn: Dr. Scott Schreck
1617 Cole Boulevard
Golden, CO 80401-3393

Prepared by

Lakshmi N. Sankar
School of Aerospace Engineering
Georgia Institute of Technology
Atlanta, GA 30332-0150

May 4, 2001

I. INTRODUCTION

A computational research program is underway at Georgia Tech in the area of horizontal-axis wind turbine aerodynamics. The research focuses on understanding the flow mechanisms that affect the performance of wind turbines in non-axial and non-uniform inflow, and the development of modern, efficient computational techniques that complement existing combined blade element-momentum theory.

The computational effort is based on the extension of a 3-D hybrid Navier-Stokes/potential flow solver that has been developed at Georgia Tech for helicopter rotor and propeller applications to horizontal axis wind turbines. In this approach three-dimensional unsteady compressible Navier-Stokes equations are solved in a small region, on a body-fitted grid surrounding the rotor blade. Away from the blades, the potential flow equation is solved. The vorticity shed by the blades as a result of dynamic stall, and the spanwise and azimuthal variations of circulation are captured using vortex filaments. These filaments are freely convected by the local flow. Since the costly Navier-Stokes calculations are done only in regions close to the wind turbine blades, and because much of the vorticity is tracked using Lagrangean techniques, this method is an order of magnitude more efficient than full blown Navier-Stokes methods.

SUMMARY OF ACTIVITIES DURING THE RESEARCH PERIOD

During this reporting period (May 6, 2000 - August 30, 2000), work was done on validating the hybrid methodology, and the full Navier-Stokes solver for a rotor tested by NREL at NASA Ames.

<u>Description of the Configuration studied</u>

This new wind turbine is referred to in NREL literature as the NREL new 10-meter wind turbine, or the Phase VI Rotor. This is a 2 bladed rotor with tapered and twisted blades. The NREL S809 airfoil was used. The rotor diameter is 10.06m. Figure 1 shows the taper and twist distribution for the blades of the Phase VI Rotor.

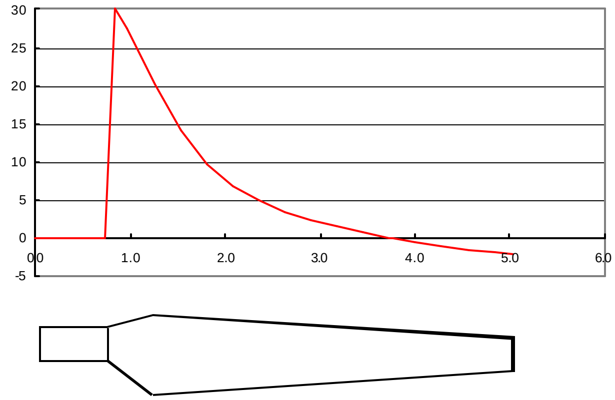

Figure 1 Twist Distribution of the Tapered/Twisted Blade for the NREL Phase VI Rotor

Results and Discussion

The data submitted in the form required by NREL was extracted by following method:

Air speeds and flow angles, at radius locations of 0.30R, 0.47R, 0.63R, 0.8R and 0.95R, and points that are 0.80c ahead of the leading edge on the chord line, were extracted by computing the sectional dynamic pressures and impinging angles. The pressure distributions at these spanwise locations were integrated to yield sectional aerodynamic forces and moments. Sectional aerodynamics coefficients were computed using the sectional dynamic pressures measured at these locations. The location where the speed and inflow angle measurements at a typical radial location are required is shown below as figure 2.

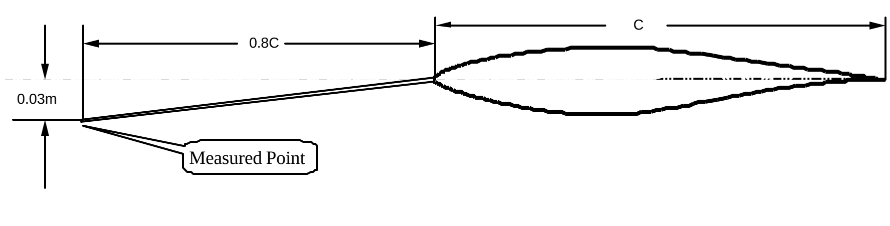

Figure 2 Velocity Measurement Location at a Typical Span-wise Location

The air speeds were interpolated at this location from CFD results. No further correction was applied. The aerodynamics coefficients and sectional loads were computed based on the equations provided by NREL in the Blind Comparison Overview. The normal force coefficients below are defined as sectional force coefficients normal to the local chord.

Figure 3 shows the normal force coefficients vs. wind speed at 95% span. A hybrid methodology was used for wind speeds 7m/s, 10m/s and 15m/s, and a full Navier-Stokes methodology was used for higher wind speeds. The results from present methodologies compare favorably with measurements.

At the time these results were submitted to NREL for blind run comparison one of the calculations, at 13m/sec wind speed had not been carried out to full convergence. These calculations have been redone, and fully converged results are shown here.

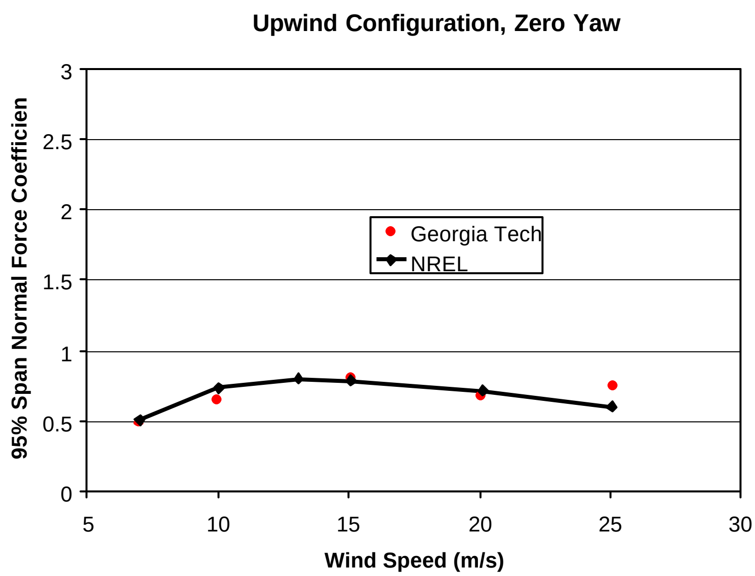

Figure 3 Normal Force Coefficients at 95% R

In our simulations, the grid is usually clustered near the tip where much of the power generation occurs. Figure 4 shows the 30% radius normal force coefficients. The grid is very sparse near the root, and the local rotating speed is much lower than the tip speed. For these reasons, the correlation between the measurements and experiments were the worst near the root.

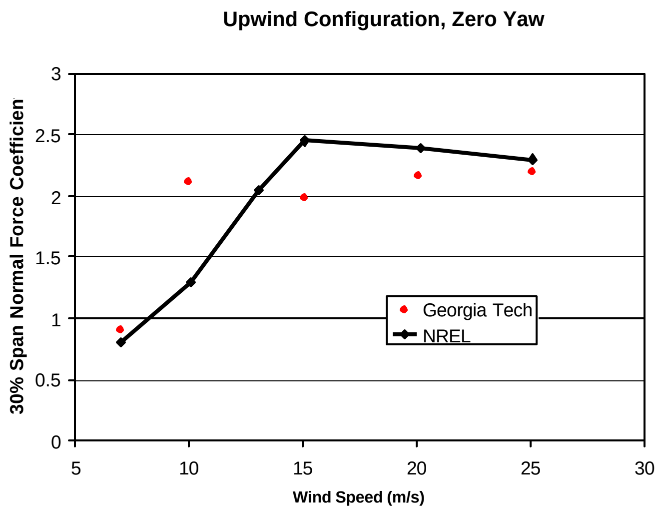

Figure 4. Normal Force Coefficients at 30% R

Figure 5 shows the flap bending moment for one of the blades at hub connection. The hybrid methodology over-predicted the flap bending moment at 10m/s, while the full Navier-Stokes methodology under-estimate the bending moment at fully stalled wind speeds.

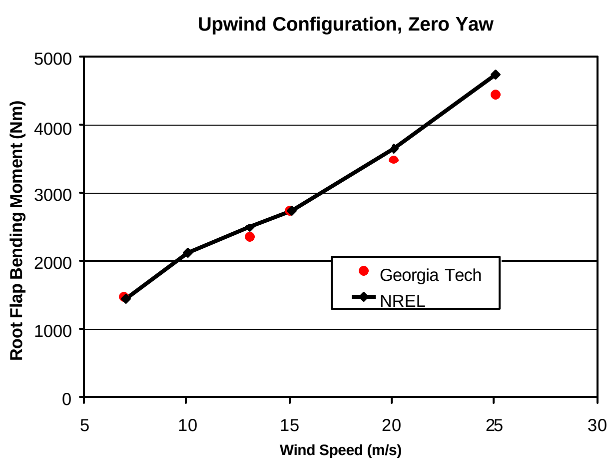

Figure 5 Flap Bending Moment variation with Wind Speed

Figure 6 shows the local dynamic pressure at 95% span location for all these cases, the Navier-Stokes simulation slightly underestimated the dynamic pressure especially at higher wind speeds.

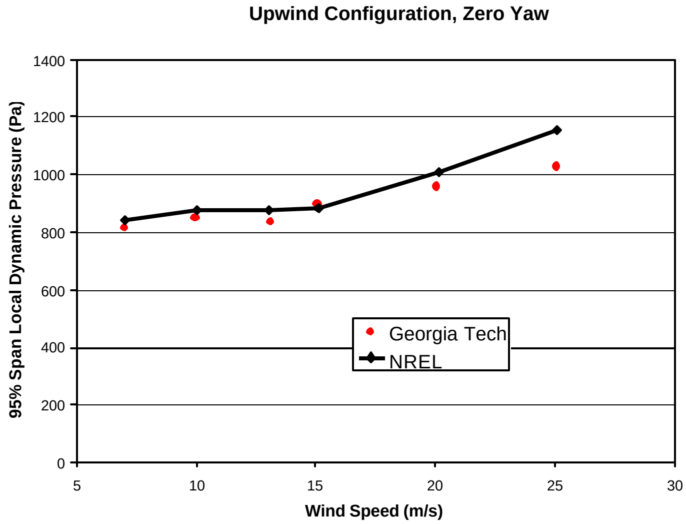

Figure 6. Computed and Measured Dynamic Pressures at 95% span